

Supplementary Materials: Selective and Efficient Olefin Epoxidation by Robust Magnetic Mo Nanocatalysts

Cristina I. Fernandes ¹, Pedro D. Vaz ^{2,3} and Carla D. Nunes ^{1,*}

¹ Centro de Química Estrutural, Departamento de Química e Bioquímica, Faculdade de Ciências, Universidade de Lisboa, 1749-016 Lisboa, Portugal; cifernandes@ciencias.ulisboa.pt

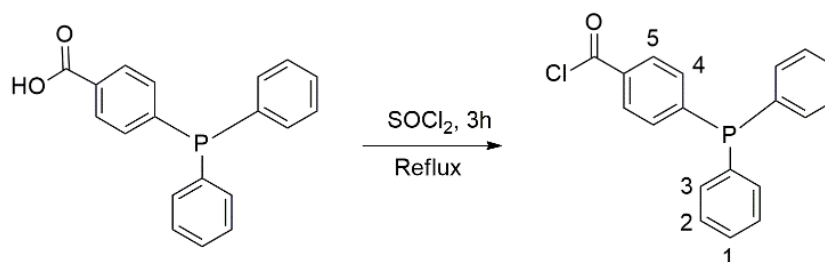
² CICECO—Aveiro Institute of Materials, Department of Chemistry, University of Aveiro, 3810-193 Aveiro, Portugal; pedro.vaz@fundacaochampalimaud.pt

³ Champalimaud Foundation, Champalimaud Centre for the Unknown, 1400-038 Lisbon, Portugal

* Correspondence: cmnunes@ciencias.ulisboa.pt

Characterization of ligand phosCl

The 4-(diphenylphosphino)benzoyl chloride (**phosCl**) ligand was prepared with a 96% yield, from the reaction between 4-(diphenylphosphino)benzoic acid (**phosOH**) and thionyl chloride (SOCl₂) according to a literature procedure [1] as shown in Scheme S1.



Scheme S1. Synthesis of 4-(diphenylphosphino)benzoyl chloride (**phosCl**) ligand.

Formation of the ligand was certified by FTIR due to the presence of a new band assigned to the $\nu_{\text{C=O}}$ mode at 1738 cm⁻¹ which is characteristic of the carbonyl group in acyl halides and due to the presence of two new bands assigned to the $\nu_{\text{C-Cl}}$ modes at 719 cm⁻¹ and 692 cm⁻¹ characteristic of acyl chloride functional group. Bands from the $\nu_{\text{C-H}_{\text{arom}}}$ mode were observed at 3010 cm⁻¹ and those from $\nu_{\text{C=C}_{\text{arom}}}$ mode were detected at 1559 cm⁻¹ and 1496 cm⁻¹ indicating the reaction success. The concomitant disappearing of the carboxylic acid bands due to OH group at 3400 cm⁻¹ (from $\nu_{\text{O-H}}$ mode) and around 1712 cm⁻¹ (from $\delta_{\text{O-H}}$) is also indicative that the reaction was accomplished.

The spectroscopic characterization of the ligand was also performed by solution NMR. The ¹H NMR spectrum of **phosCl** ligand exhibits peaks at δ values of 8.22 (H₅), 7.87 (H₁), 7.70 (H₂), 7.64 (H₄) and 7.55 (H₃) ppm assigned to the protons of the heteroaromatic ring. These δ values are different from the corresponding carboxylic acid that showed peaks at 11.0 (OH), 8.48 (H₅), 7.78 (H₂ and H₁), 7.57 (H₄) and 7.36 (H₃) ppm, confirming the reaction success.

Characterization and performance of magnetic nanoparticles

Powder XRD

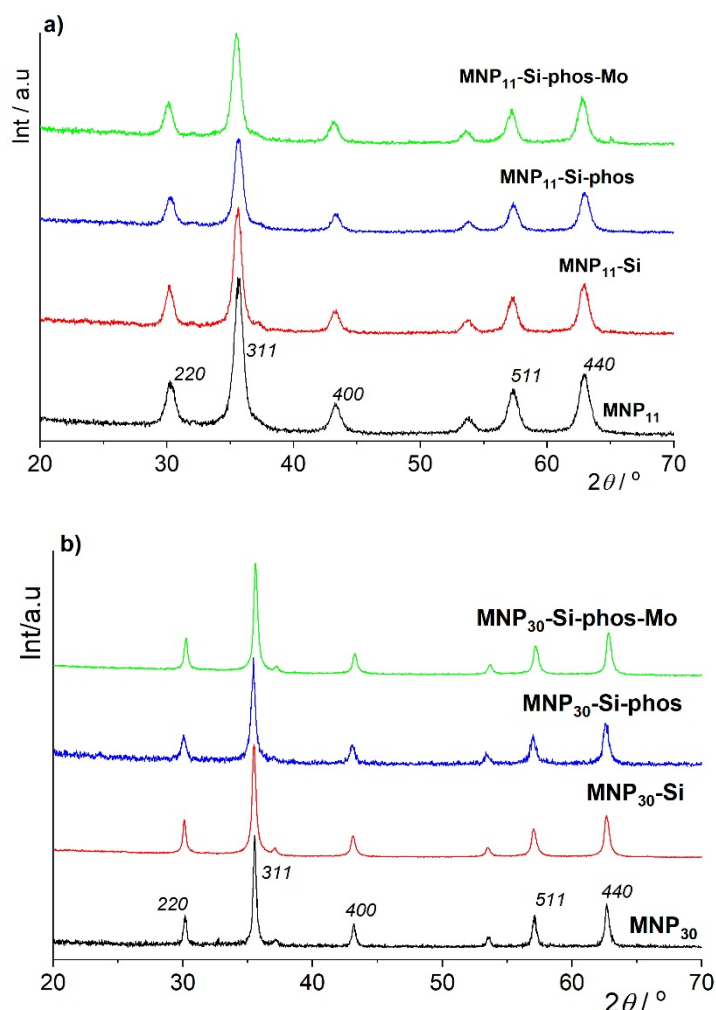


Figure S1. XRD powder patterns of all prepared materials starting from **MNP₁₁** (a) and **MNP₃₀** (b). Indexation of the most relevant magnetite (Fe_3O_4) plans is also shown.

SEM-EDX

SEM images show that **MNP₃₀** (Figure S2a) exhibited aggregated spherical particles having rough external surfaces, and after silica coating the resulting **MNP₃₀-Si** nanoparticles (Figure S2b) exhibited smooth and spongy surface showing the successful coating of the magnetic nanoparticles with silica. The aggregation of nanoparticles increased after the subsequent reactions, namely, coordination of the ligand and the metal precursor.

By comparison, analyzing the SEM image of the **MNP₃₀-Si_{us}** nanoparticles (Figure S2c) it was possible to observe that the particles were sphere and aggregated and they also had a smooth and spongy surface displaying that the coating of the magnetic nanoparticles with silica was successful as well. However, Figure S2c also evidences that the SEM image shows more defined contours in the nanoparticles synthesized by this ultrasound route for the Stöber method as compared to those prepared via the traditional mechanical stirring (Figure S2b).

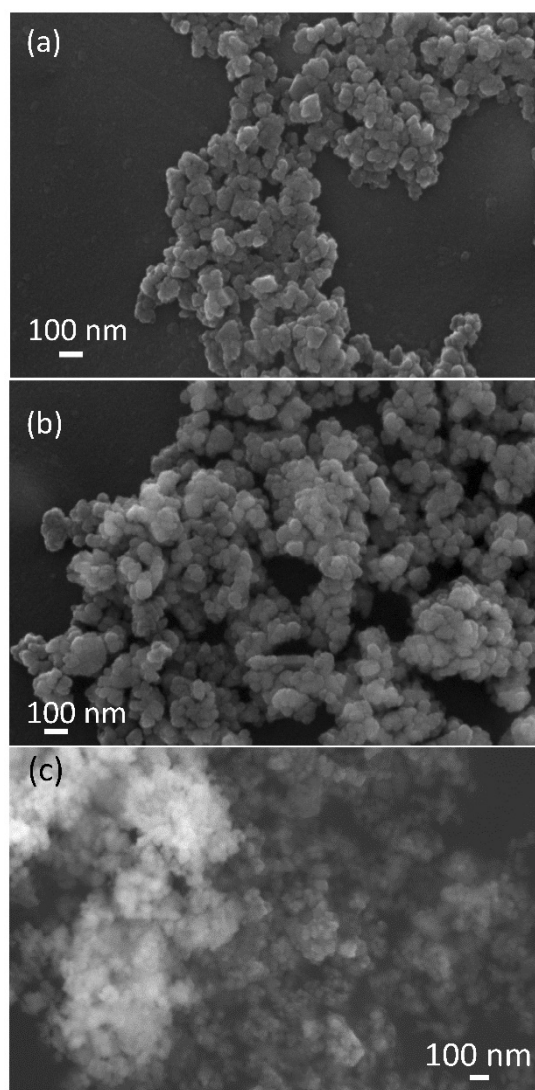


Figure S2. SEM images of **MNP₃₀** (a), **MNP₃₀-Si** (b) and **MNP₃₀-Si_{us}** (c).

Figure S3a presents the Energy dispersive X-ray (EDX) spectrum of the **MNP₃₀-Si** nanoparticles in which Fe, O and Si, were all present, after the grafting reaction. Figure S3b presents the EDX for material **MNP₃₀-Si-phos-Mo** (Figure S3b) where iron, silicon, carbon, nitrogen and molybdenum were detected in the sample, which confirmed the successful anchoring of the active sites.

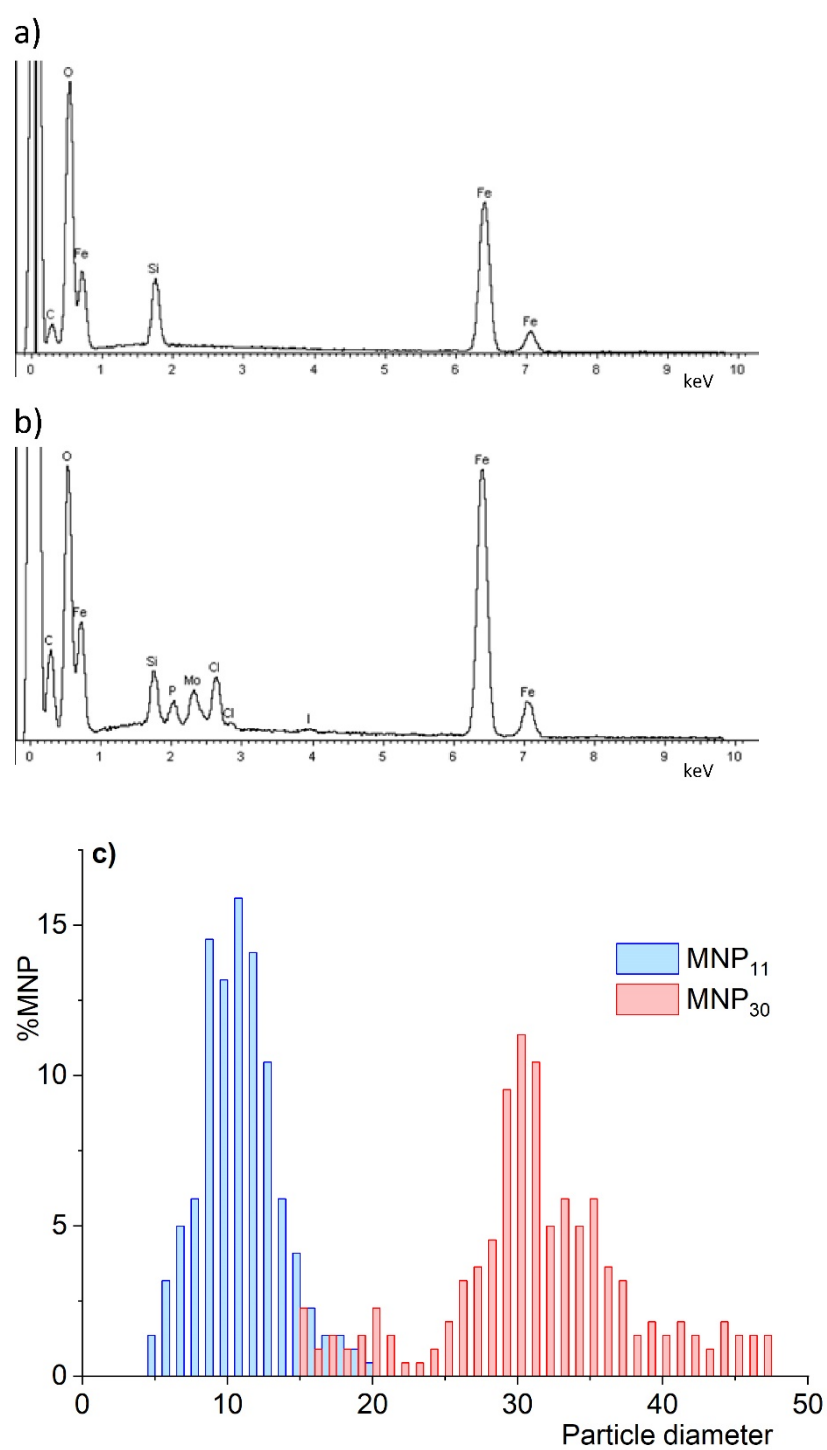


Figure S3. EDX spectra of MNP₃₀-Si (a), MNP₃₀-Si-phos-Mo (b) and the particle size distribution histograms for both MNP₁₁ and MNP₃₀ based on TEM measurements (c).

FTIR

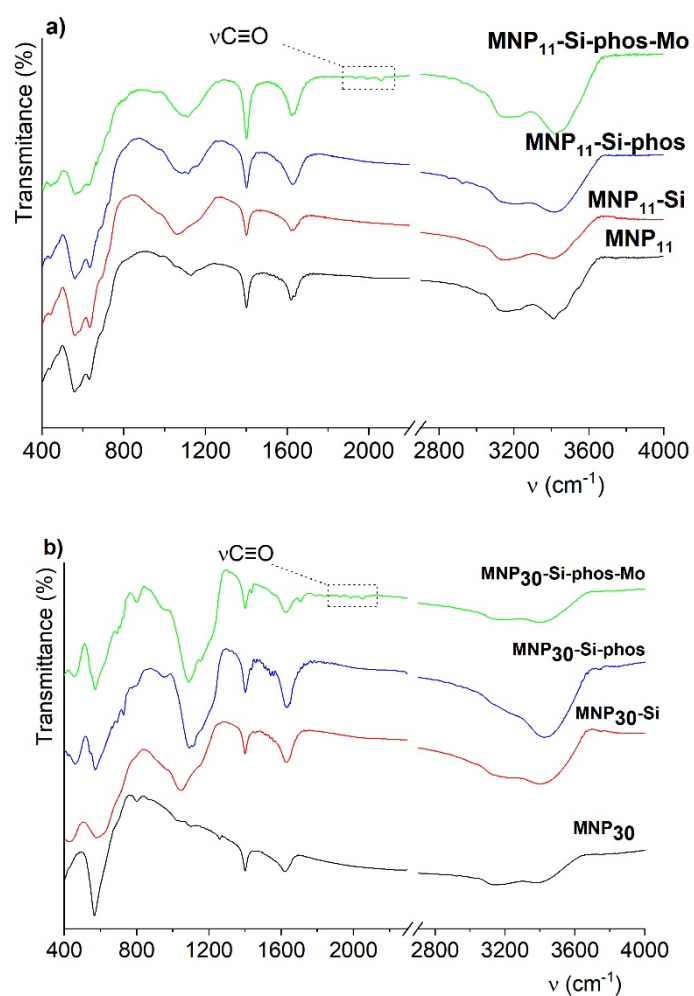
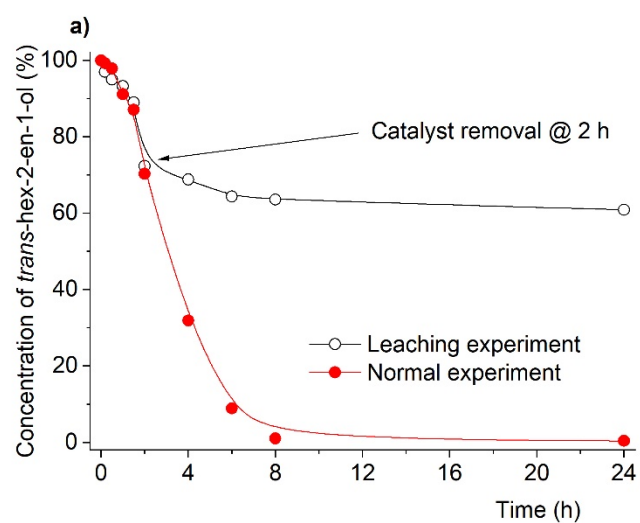


Figure S4. FTIR spectra of MNP_{11} (a) and MNP_{30} by mechanical stirring route (b) derived materials. The dotted boxes highlight the $\nu C\equiv O$ modes denoting presence of the $[MoI_2(CO)_3]$ moiety.

Leaching experiments



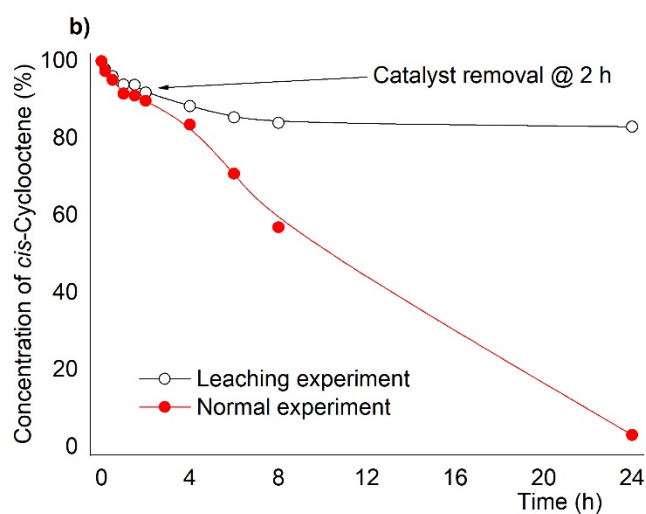


Figure S5. Leaching experiment reaction kinetics of substrate consumption in toluene at 353 K for (a) *trans*-hex-2-en-1-ol using **MNP₁₁-Si-phos-Mo** and (b) *cis*-cyclooctene using **MNP₃₀-Si_{us}-phos-Mo** as catalysts, respectively. In both experiments, catalysts were removed after 2 h reaction time.

References

1. Ventura, A.C.; Fernandes, C.I.; Saraiva, M.S.; Nunes, T.G.; Vaz, P.D.; Nunes, C.D. Tuning the Surface of Mesoporous Materials Towards Hydrophobicity-Effects in Olefin Epoxidation. *Curr. Inorg. Chem.* **2011**, *1*, 156-165, doi: 10.2174/1877944111101020156